Spatio-Temporal Wireless D2D Network With Imperfect Beam Alignment

Yibo Quan, Marceau Coupechoux, Jean-Marc Kelif

Spatio-Temporal Wireless D2D Network With Imperfect Beam Alignment

Yibo Quan ‡ §, Marceau Coupechoux‡ and Jean-Marc Kélif §
‡ LTCI, Télécom Paris, Institut Polytechnique de Paris, 91120, Palaiseau, France
§Orange Labs, 92320, Châtillon, France
Email: {yibo.quan, marceau.coupechoux}@telecom-paris.fr, {jeanmarc.kelif}@orange.com

***Abstract*—In this paper, we investigate the beam misalignment impacts of a dynamic device-to-device (D2D) communication model, where both transmitters and receivers adopt beamforming (BF) by using uniform linear array (ULA). A time continuous dynamic model is adopted for this network. We use tools of stochastic geometry and the Miyazawa rate conversation law to analyse the stability condition of such a network. An analytical expression of the critical arrival rate is given under a uniform or truncated Gaussian alignment error assumption. In contrast to our previous result, where the beam alignment is perfect, our analytical and numerical results show that, if the beam alignment is not perfect, the critical arrival rate can no longer increase without limit as a function of the number of antenna elements. Closed-form expressions of the upper bounds for critical arrival rates are given for both the uniform and the truncated Gaussian misalignment models.**

***Index Terms*—Stochastic geometry, birth-death process, beamforming, stability, device-to-device, misalignment.**

I. Introduction

As a promising technology to meet the unparalleled explosion of demands for high data rate services, device-to-device (D2D) communication has attracted considerable attention to improving the quality of service (QoS) of proximity services needs. An essential challenge of D2D networks is the management of co-channel interference. To tackle this problem, the adoption of BF in the millimeter-wave band is studied by multiple authors [1]–[3]. Among these works, a classical antenna configuration, namely the uniform linear array (ULA) [3], is widely adopted.

Most existing works that study the QoS of D2D communication focus on the analysis of rate and coverage [1] [4]. These works study the average performance of the network, given a static configuration of device locations. The methods of stochastic geometry are applied in these studies. Some works study more dynamic cases [5] [6], where each device has a dynamic queue of packets to transmit. In these works, networks are modeled as classical queue interacting problems [7], and time is slotted and thus considered as discrete. A weakness of this model lies in the constant number of users throughout time. In a more realistic network model, users arrive at random locations, at random time instants, with a random amount of data to be transmitted and leave the network when the transmission is over. Thus, a spatial birth-death wireless network [8] is proposed to model this network as a continuous-time spatial birth-death process [9]. The stability condition of this network is given in [8]. In [3], we extend this result to a D2D network equipped with directional antenna arrays. An expression for the critical arrival rate is provided, i.e., the user arrival rate below which the network is stable.

Similar to many other works, we assume that the beam directions of the associated transmitter-receiver pairs are perfectly aligned in [3]. However, due to the estimation errors of the directions and other hardware limitations, the beam alignment error (BAE) cannot be neglected. Paper [10] shows that for a Poisson bipolar network, the BAE can significantly impact the throughput and the coverage. Similar works are done to evaluate the coverage and rate performance of D2D or cellular networks in the presence of BAE [11] [12]. Besides the flat-top antenna power pattern model proposed in [3], paper [10] also models the directional antenna pattern using a cosine function to obtain a more accurate array power pattern. A uniform BAE model and a Gaussian BAE model are studied in [10] and [11].

In this paper, we extend the results of [3] to D2D networks with imperfect beam alignment. The contribution of this paper can be summarized as follows:

- We propose a uniform BAE model and a truncated Gaussian BAE model for continuous-time spatial birth-death D2D networks, where the realistic power pattern of ULA is considered.
- We derive new critical arrival rates for this D2D network as a function of the number of antenna elements by considering the aforementioned BAE models. A closed-form expression of the critical arrival rate's upper bound for each BAE model is given.
- Our analytical and numerical results show that beam misalignment reduces the stability region of D2D networks with BF. Although we confirm that the critical rate is an increasing function of the number of antennas, we highlight an upper bound which depends on the antenna alignment error amplitude.

In the rest of this paper, we introduce the system models in section II. Section III presents the stability criteria. Section IV derives upper bounds of the critical arrival rate. The numerical results are shown in section V. Section VI concludes the paper.

The work of M. Coupechoux is performed at LINCS laboratory.

II. System Model

A. Spatial Birth-Death Process

The spatial birth-death process is a generalized birth-death process that considers the spatial locations of the individuals. Specifically, the birth rate and the death rate of the process depend on the spatial configuration of the individuals at each time instant. For example, consider a 2-dimension Poisson dipole network, where the transmitter-receiver D2D user pairs live in a two-dimensional Euclidean plane $\mathbf{S}$, $\mathbf{S} \subset \mathbb{R}^2$. Each transmitter has a file of random size to transmit to its associated receiver. This network is categorized as a birth-death process since the time instants at which it appears and leaves the network are random for each pair. We use the Poisson process with arrival rate $\lambda|\mathbf{S}|$ to model the 'birth' (or arrival) time instants of the transmitter-receiver pairs, where $\lambda \in \mathbb{R}^+$ is the arrival rate per unit of area.

Once a pair appears in the network, it starts the file transmission. For all the pairs, the file size is assumed to be an i.i.d. random variable following an exponential law of mean L bits. The transmission rate of each pair is dynamic following the Shannon rate, where the interference comes from other active pairs. When the transmission is finished, the pair leaves the network immediately. Moreover, the appearing positions of the transmitter-receiver pairs also form a homogeneous Poisson point process. We assume that the transmitter devices are uniformly distributed on the disks centered around the receivers of radius T, where T is supposed to be a constant in our studies.

The spatial birth-death process is known to be a continuous-time Markov chain (CTMC) [9], whose states are the position configurations of the pairs. At each time instant t, the positions of pairs can be interpreted as a marked point process $\Phi_t = \sum_{i=1}^{N_t} \delta(x_i, y_i)$, where $N_t = \Phi_t(\mathbf{S})$ is the number of active pairs in the plane at time t; x_i denotes the position of the i-th active receiver; the mark y_i denotes the transmitter location of the i-th pair; $\delta(\cdot)$ is the Dirac measure. Thus the process $\Phi_t(\mathbf{S})$ is a classical birth-death process defined as a counting measure.

B. Beamforming

Similar to the BF model in our previous work [3], we consider a point-to-point system in free-space with line-of-sight (LOS) propagation. Both the transmitter and the receiver sides are equipped with 1-dimensional ULA. For each array, n antenna elements are aligned along a straight line and are uniformly spaced with distance d. Considering the arrays at the transmitter side first, in the direction θ with respect to the axis of ULA, the far-field pattern f_a^T of the array is the sum of n plane waves emitted by each element:

$$f_a^T(\theta) \quad = \quad \frac{1}{\sqrt{n}} f_e(\theta) \sum_{i=1}^{n} a_i e^{j((i-1)kd\cos\theta)} \qquad (1)$$

where $f_e(\theta)$ is the field pattern at every antenna element; $k = 2\pi/\lambda$ where λ is the wavelength and a_i is a phase offset applied at antenna element i. The term $1/\sqrt{n}$ is a normalization factor to account for the power split among the n antenna elements. Let θ_0^T be the chosen boresight direction of the transmitter's antenna array. Choosing $a_i = e^{-j((i-1)kd\cos\theta_0^T)}$, the power gain $g_a^T(\theta, \theta_0^T) = |f_a^T(\theta)|^2$ is given by:

$$g_a^T(\theta, \theta_0^T) \quad = \quad \frac{1}{n} g_e(\theta) \left| \frac{\sin(nk\frac{d}{2}(\cos\theta - \cos\theta_0^T))}{\sin(k\frac{d}{2}(\cos\theta - \cos\theta_0^T))} \right|^2 \qquad (2)$$

where $g_e(\theta)$ is the power pattern of an antenna element. If we assume a rectangular patch antenna, the antenna radiation pattern is hemispheric and has a directivity of 2 [13]. Hence, we now assume $d = \lambda/2$ and g_e defined as follows:

$$g_e(\theta) = \begin{cases} 2, & \theta \in [0, \pi] \\ 0, & \text{otherwise} \end{cases} \qquad (3)$$

The maximum array factor gain for the transmitter is achieved for $\theta = \theta_0^T$ [14]. Thus, the maximum gain of the transmitters antenna is $g_a^T(\theta_0^T, \theta_0^T) = 2n$.

Now for the receiver antenna, there is no need to divide the power into n parts. So the power of the received signal is given by:

$$g_a^R(\theta, \theta_0^R) \quad = \quad g_e(\theta) \left| \frac{\sin(nk\frac{d}{2}(\cos\theta - \cos\theta_0^R))}{\sin(k\frac{d}{2}(\cos\theta - \cos\theta_0^R))} \right|^2 \qquad (4)$$

Similarly, the maximum array factor gain is achieved for $\theta = \theta_0^R$. We use the same value of g_e as in (3). Then, the maximum gain is $g_a^R(\theta_0^R, \theta_0^R) = 2n^2$.

C. Beam alignment error distribution

We now align the direction of the array's maximum radiation at the transmitter side to the direction of its associated receiver by setting θ_0^T to be the angle of departure (AoD) ξ with respect to the array's axis. At the receiver side, we set $\theta_0^R = \psi$ to align the main beam of the receiver towards its transmitter, where ψ is the angle of arrival (AoA) concerning the axis of ULA. To simplify the calculation, we suppose that all the antenna arrays are set to be broadside array antennas, where $\theta_0^T = \theta_0^R = \pi/2$. Devices then try to adjust their directions so that the axes of the corresponding antenna arrays are parallel to each other and the main lobes are aligned with each other. However, due to potential errors in the estimation of AoD and AoA, the main antenna lobes may not be perfectly aligned (see Fig. 1, where the BAE is denoted as e). Hence, we assume that ξ and ψ are two random variables with the same mean of $\pi/2$. In other words, we suppose that there are estimation errors for the exact directions of the devices. The center of the error regions is the main beam directions of the concerned devices. Moreover, the alignment error distribution is supposed to be identical not only for both transmitter and receiver sides but also for all the device pairs. This assumption is reasonable since all the devices are, i.i.d. distributed with similar environmental conditions in the network.

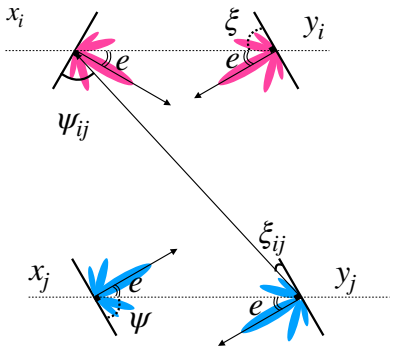

Fig. 1. Two D2D transmitter-receiver pairs at $[x_i, y_i]$ and $[x_j, y_j]$. For each receiver/transmitter, ψ/ξ represents the AoA/AoD of the plane wave from/to the corresponding transmitter/receiver, which has an error difference e with its maximum radiation direction (broadside direction in the figure). ψ_{ij}/ξ_{ij} is the direction of interfering transmitter/receiver.

Denote the probability density function (pdf) of ξ as f_ξ and the pdf of ψ as f_ψ. Then the mean of transmitter's antenna gain in the direction ξ is:

$$\mathbb{E}[g_a^T(\xi, \theta_0^T)] = \int_{-\pi}^{\pi} g_a^T(x, \theta_0^T) f_\xi(x) \mathrm{d}x \tag{5}$$

The mean of the receiver's antenna gain at the direction ψ is:

$$\mathbb{E}[g_a^R(\psi, \theta_0^R)] = \int_{-\pi}^{\pi} g_a^R(x, \theta_0^R) f_\psi(x) \mathrm{d}x \tag{6}$$

Two BAE distributions are studied in this paper, namely the uniform distribution and the truncated Gaussian distribution.

1) Uniform Beam Alignment Error: We assume that the error occurs with the same likelihood in a certain error region. This model is used where only some preliminary information about the error limits is known. Thus we have $\xi \sim U(\theta_0^T - \epsilon, \theta_0^T + \epsilon)$ and $\psi \sim U(\theta_0^R - \epsilon, \theta_0^R + \epsilon)$, where ϵ is the error limit.

2) Truncated Gaussian Beam Alignment Error: According to the central limit theorem, the Gaussian distribution can properly estimate the beam errors induced by multiple independent sources. We assume that the errors have a span from $-\pi$ to π. The PDF of ξ can be expressed by using the truncated Gaussian distribution [15]:

$$f_\xi(x) = \frac{1}{\sqrt{2\pi}\sigma} \frac{\exp(-\frac{1}{2}(\frac{x-\theta_0^T}{\sigma})^2)}{erf(\frac{\pi}{\sqrt{2}\sigma})}, x \in [\theta_0^T - \pi, \theta_0^T + \pi] \tag{7}$$

Similarly, we have $f_\psi(x)$ of the same form:

$$f_\psi(x) = \frac{1}{\sqrt{2\pi}\sigma} \frac{\exp(-\frac{1}{2}(\frac{x-\theta_0^R}{\sigma})^2)}{erf(\frac{\pi}{\sqrt{2}\sigma})}, x \in [\theta_0^R - \pi, \theta_0^R + \pi] \tag{8}$$

where $erf(\cdot)$ is the Gaussian error function defined as $erf(x) = \frac{2}{\sqrt{\pi}} \int_0^x e^{-t^2} \mathrm{d}t$.

D. Transmission Rate

Consider a Line-of-Sight propagation environment with no multi-path fading. We denote the path-gain function as $\ell(\cdot) : \mathbb{R} \to \mathbb{R}$. All the transmitter devices use the same frequency and have the same transmission power P. Let G_{ij}^T denote the antenna gain of a transmitter located at y_j, in the direction of a receiver located at x_i. The corresponding antenna gain of the receiver at x_i for the same path is denoted as G_{ij}^R. As shown in Fig. 1, for a plane wave departing from y_j towards x_i, the AoD and the AoA with respect to the axis of ULA are denoted as ξ_{ij} and ψ_{ij}, respectively. Hence we have $G_{ij}^T = g_a^T(\xi_{ij}, \theta_0^T)$ and $G_{ij}^R = g_a^R(\psi_{ij}, \theta_0^R)$. Thus the interference at a receiver located at x_i leads to:

$$I^{BF}(x_i, \Phi_t) = \sum_{[x_j, y_j] \in \Phi_t, i \neq j} G_{ij}^T G_{ij}^R P \ell(\|x_i - y_j\|) \tag{9}$$

Let B denote the bandwidth and $\mathcal{N}_0$ denotes the noise power. The expression of the transmission rate for pair at $[x_i, y_i]$ is:

$$R^{BF}(x_i, \Phi_t) = B \log_2 \left(1 + P \frac{G_{ii}^R G_{ii}^T \ell(T)}{\mathcal{N}_0 + I^{BF}(x_i, \Phi_t)}\right) \tag{10}$$

Note that $G_{ii}^T = g_a^T(\xi, \theta_0^T)$ and $G_{ii}^R = g_a^R(\psi, \theta_0^R)$.

III. Stability Criterion

Since a spatial birth-death process can be characterized as a Markov chain, it is crucial to know whether it has a stationary regime. The critical arrival rate λ_c is defined as the threshold of arrival rate such that the spatial birth-death process Φ_t is stable if and only if $\lambda < \lambda_c$. In [8], a closed-form expression of the critical rate is given for the network that we describe in section II-A without BF:

$$\lambda_c = \frac{B\ell(T)}{\ln(2) L a}, \tag{11}$$

where $a = \int_{\mathbf{S}} \ell(\|x\|) dx$. In other words, all the users in such a network can finish their file transmissions within the limit time interval, if and only if $\lambda < \lambda_c$. Otherwise, the system is unstable and the number of active pairs tends to infinity.

In [3], a critical arrival rate under the BF paradigm in section II-B is given for the case without misalignment:

$$\lambda_c^{BF}(n) = \frac{G_{max}^R G_{max}^T B\ell(T)}{\ln(2) L \mathbb{E}[a^{BF}]} \tag{12}$$

where $G_{max}^R = 2n^2$ and $G_{max}^T = 2n$. $\mathbb{E}[a^{BF}]$ is the integral over $\mathbf{S}$ of the path-gain function amplified with BF:

$$\mathbb{E}[a^{BF}] = \frac{a}{4\pi^2} \int_{-\pi}^{\pi} g_a^T(\theta, \theta_0^T) \mathrm{d}\theta \int_{-\pi}^{\pi} g_a^R(\eta, \theta_0^R) \mathrm{d}\eta \tag{13}$$

In this paper, we extend the stability criteria to the network where the alignment error is considered. The new critical arrival rate can be expressed as follows:

$$\hat{\lambda}_c^{BF}(n) = \frac{\mathbb{E}[g_a^T(\xi, \theta_0^T)] \mathbb{E}[g_a^R(\psi, \theta_0^R)] B\ell(T)}{\ln(2) L \mathbb{E}[a^{BF}]} \tag{14}$$

where $\mathbb{E}[g_a^T(\xi,\theta_0^T)]$ and $\mathbb{E}[g_a^R(\psi,\theta_0^R)]$ are given by (5) and (6), which are functions of n.

Theorem 1. Assuming the ULA model with n antenna elements, when there is beam alignment error, the spatial birth-death process Φ_t admits no stationary regime if $\lambda > \hat{\lambda}_c^{BF}(n)$.

Proof: See Appendix A.

IV. Performance Analysis

As shown in [3], the critical arrival rate rises rapidly as a function of the number of antenna elements n if there is no BAE. For the extreme case, λ_c^{BF} can increase to infinity when n tends to infinity. In contrast to this result, we will show that the critical arrival rate $\hat{\lambda}_c^{BF}$ can no longer increase without limit, considering the imperfect beam alignment.

A. Uniform Beam Alignment Error

When the error is limited in a region $[-\epsilon,\epsilon]$ and $\theta_0^T = \theta_0^R = \frac{\pi}{2}$, the critical arrival rate can be expressed as follows:

$$\hat{\lambda}_c^{BF}(n) = \begin{cases} \dfrac{\pi^2\lambda_c}{\epsilon^2}\left(\dfrac{\int_{\pi/2-\epsilon}^{\pi/2+\epsilon}\left|\frac{\sin(\frac{1}{2}n\pi\cos\theta)}{\sin(\frac{1}{2}\pi\cos\theta)}\right|^2 \mathrm{d}\theta}{\int_0^{\pi}\left|\frac{\sin(\frac{1}{2}n\pi\cos\theta)}{\sin(\frac{1}{2}\pi\cos\theta)}\right|^2 \mathrm{d}\theta}\right)^2, \epsilon \le \pi/2 \\ \dfrac{\pi^2\lambda_c}{\epsilon^2}, \quad \epsilon > \pi/2 \end{cases} \tag{15}$$

Since the part in the brackets is less than 1, the critical arrival rate λ_c^{BF} has an upper bound:

$$\hat{\lambda}_c^{BF}(n) \le \frac{\pi^2\lambda_c}{\epsilon^2} \tag{16}$$

B. Truncated Gaussian Beam Alignment Error

When the errors have distributions given by (7) and (8), the critical arrival rate can be expressed as follows:

$$\hat{\lambda}_c^{BF}(n) = \frac{2\pi\lambda_c}{\sigma^2 erf^2(\frac{\pi}{\sqrt{2}\sigma})} \times \left(\frac{\int_0^{\pi}\left|\frac{\sin(\frac{1}{2}n\pi\cos\theta)}{\sin(\frac{1}{2}\pi\cos\theta)}\right|^2 \exp(-\frac{1}{2}(\frac{\theta-\frac{\pi}{2}}{\sigma})^2)\mathrm{d}\theta}{\int_0^{\pi}\left|\frac{\sin(\frac{1}{2}n\pi\cos\theta)}{\sin(\frac{1}{2}\pi\cos\theta)}\right|^2 \mathrm{d}\theta}\right)^2 \tag{17}$$

Since the exponential coefficient in the brackets is non-negative and less than 1, $\hat{\lambda}_c^{BF}$ has an upper bound as follows:

$$\hat{\lambda}_c^{BF}(n) \le \frac{2\pi\lambda_c}{\sigma^2 erf^2(\frac{\pi}{\sqrt{2}\sigma})} \tag{18}$$

V. Simulation

In this section, we numerically illustrate our theoretical results. Our simulator works on a square plane $\mathbf{S} = [-Q,Q]^2, Q \in \mathbb{R}^+$. As explained in section II-A, there are two types of events in a spatial birth-death process: arrivals of new device pairs and departures of pairs that have finished their transmissions. The configuration of Φ_t only changes when these two events arise, so do the transmission rates of the device pairs. The 'birth' events follow a Poisson process of rate $\lambda|\mathbf{S}|$, so the inter-arrival time t_a follows the exponential law of mean $\frac{1}{\lambda|\mathbf{S}|}$ in seconds. The time interval t_d from time t to the next 'death' is estimated as the minimum delay that any pair finishes its file transmission using the transmission rate imposed by Φ_t. So the mechanism of the simulator states that, after each 'birth' event, we compare t_a and t_d. Once t_a is less than t_d, we add a new device pair at a random position in $\mathbf{S}$. Otherwise, we delete the pair that finishes its transmission. We then update the transmission rates, the remaining file sizes, and the time interval to the next 'birth' or 'death'. The total number of active pairs $\Phi_t(\mathbf{S})$ and the time t are recorded when these events occur. For each pair, we adopt (10) to calculate the transmission rate. The AoDs ξ and AoAs ψ are set to be random variables whose means are θ_0^T and θ_0^R ($\theta_0^T = \theta_0^R = \pi/2$).

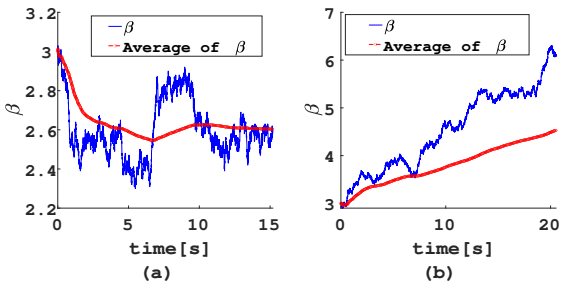

Fig. 2. System intensity β as a function of time for network with Uniform beam alignment error. (a) $\lambda = 0.9\hat{\lambda}_c^{BF}$; (b) $\lambda = 1.1\hat{\lambda}_c^{BF}$, where $\epsilon = 0.2\pi$, $n = 4$, $\hat{\lambda}_c^{BF} = 1.8258$ ($\lambda_c^{BF} = 12.9721$ without misalignment).

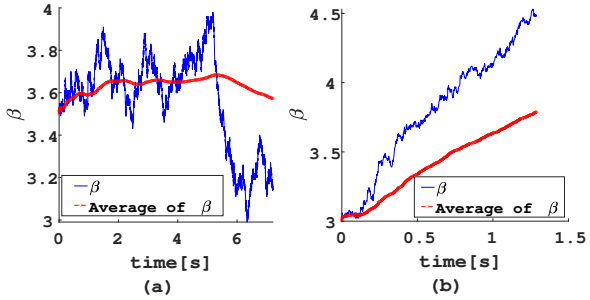

Fig. 3. System intensity β as a function of time for network with truncated Gaussian beam alignment error. (a) $\lambda = 0.9\hat{\lambda}_c^{BF}$; (b) $\lambda = 1.1\hat{\lambda}_c^{BF}$, where $\sigma = 0.3$, $n = 4$, $\hat{\lambda}_c^{BF} = 3.7737$ ($\lambda_c^{BF} = 12.9721$ without misalignment).

In our simulation, we take a bounded path-loss model $\ell(r) = (1+r)^{-4}$. The system intensity β is a critical measure to evaluate the stability of the process. Generally speaking, $\beta(t)$ is defined as the density of user pairs per unit area at time t: $\beta(t) = \frac{\Phi_t(\mathbf{S})}{|\mathbf{S}|}$. We say that the system is stable if and only if $\beta(t)$ doesn't grow indefinitely to infinity. In Fig. 2, we show $\beta(t)$ as a function of time (blue curves), and the moving average of $\beta(t)$ (red curves), where the uniform BAE is taken into account. The critical arrival rate $\hat{\lambda}_c^{BF}$ is calculated using (18), by considering the same values of parameters as in [3]. It is shown in Fig. 2(a) that $\beta(t)$ doesn't grow indefinitely to infinity when λ is less than $\hat{\lambda}_c^{BF}$, which illustrates that Φ_t is stable. Fig. 2(b) shows that the population of active pairs in

the plane and β tends to infinity when $\lambda > \hat{\lambda}_c^{BF}$. Thus, we confirm the result of Theorem 1 and the expression of $\hat{\lambda}_c^{BF}$ in (18). In the same way, we confirm the expression of the critical arrival rate $\hat{\lambda}_c^{BF}$ given in (17) by Fig. 3, under the assumption of a truncated Gaussian BAE.

Fig. 4 and 5 show the ratio between the critical arrival rate with BF $\hat{\lambda}_c^{BF}$ and without BF λ_c for the uniform and truncated Gaussian BAE models, respectively. The solid red curve assumes a perfect alignment of beams; it is increasing and tends to infinity as the number of antenna elements increases to infinity as well. This is due to the fact that when n increases, the maximum antenna array gain increases and, as the beam becomes thinner, interference is reduced. When a beam alignment error is assumed, the ratio is still increasing, but it is also upper bounded by and tends toward a value that depends on the magnitude of the error. The larger the magnitude of the error, the lower the upper limit. Suppose the error is too high (typically when $\epsilon > \frac{\pi}{2}$), BF performance is close to the performance with omnidirectional antennas. We observe that when n increases, even a tiny misalignment error degrades the performance significantly. This is due to the fact that beams are becoming thinner and thinner as n increases, and a slight angle variation implies a drop in the antenna gain. We conclude that the spatial multiplexing gain of ULA is limited when the beam alignment is not perfect.

Fig. 6 illustrates that under the context of uniform misalignment, $\hat{\lambda}_c^{BF}$ decreases when we extend the size of the error region. When $\epsilon = \pi$, the difference between the broadside direction and the AoD/AoA of the associated device can be any value between $[0, 2\pi]$. The arrival rate that the system can support is the same as with a single antenna system in this case ($\hat{\lambda}_c^{BF}/\lambda_c$ tends to 1). For the Gaussian misalignment, the impact of normal deviation σ is studied in Fig. 7. When σ is very large, the BF pattern can no longer aggregate the power to the directions of devices. The critical arrival rate with ULA decreases towards λ_c with a single antenna as a function of σ.

VI. Conclusion

This paper studies the impacts of misalignment for a spatial wireless D2D network equipped with ULA. Both the uniform beam alignment error model and the truncated Gaussian beam alignment error model are studied. The network is modeled as a spatial birth-death process, which combines stochastic geometry ideas and the queuing theory methods. Our main contribution is to establish the closed-form expression for the network's critical arrival rate as a function of the number of antenna arrays' elements by considering the misalignment models mentioned above. We derive an upper bound of the critical arrival rate for each misalignment model. Even though the number of antenna elements increases, the critical arrival rate cannot exceed these upper bounds. The numerical results show that these upper bounds match properly when the number of antenna elements is large enough.

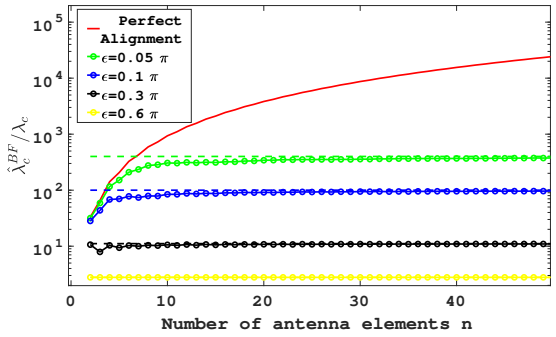

Fig. 4. λ_c^{BF}/λ_c for network with perfect alignment (red curve); $\hat{\lambda}_c^{BF}/\lambda_c$ as a function of n for network with Uniform BAE (curves with circle marks); Upper bounds of $\hat{\lambda}_c^{BF}/\lambda_c$ for different error regions ϵ (dotted lines).

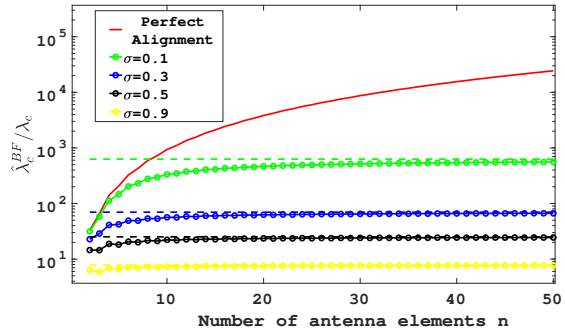

Fig. 5. λ_c^{BF}/λ_c for network with perfect alignment (red curve); $\hat{\lambda}_c^{BF}/\lambda_c$ as a function of n for network with Gaussian BAE (curves with circle marks); Upper bounds of $\hat{\lambda}_c^{BF}/\lambda_c$ for different normal deviations σ (dotted lines).

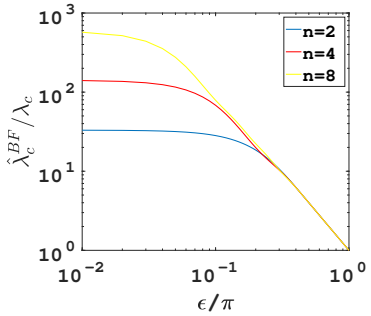

Fig. 6. $\hat{\lambda}_c^{BF}/\lambda_c$ as a function of ϵ/π for network with Uniform BAE.

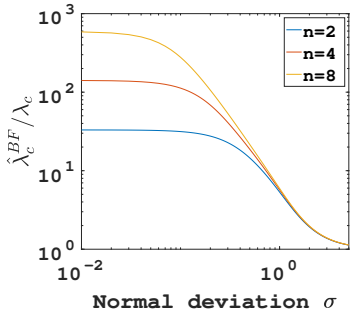

Fig. 7. $\hat{\lambda}_c^{BF}/\lambda_c$ as a function of σ for network with Gaussian BAE.

APPENDIX A

The procedures to prove the stability condition is the same as in [3]. The only difference is induced by the change of antenna gain functions. To prove the theory, we apply the Miyazawa's rate conservative law (RCL) [16], which states that the average rates of increase should be equal to the rates of decrease for a stationary stochastic process. By applying RCL to the counting measure $\Phi_t(\mathbf{S})$, we get the relation:

$$\lambda|\boldsymbol{S}| = \lambda_d. \tag{19}$$

Where λ_d is the departure rate. Denote Φ_0 as the process when Φ_t is stable. By considering the total volume of data that visit the network, the RCL leads to:

$$\lambda|\boldsymbol{S}|L = \mathbb{E}\left[\sum_{x\in\Phi_0} R^{BF}(x,\Phi_0)\right] \tag{20}$$

Next we apply the RCL to the sum interference in the network, which is denoted as $\mathbf{I}_t^{BF} = \sum_{x\in\Phi_t} I^{BF}(x,\Phi_t)$. Let $\mathcal{I} = \mathbf{I}_{0+} - \mathbf{I}_0$ denotes the additional interference arisen by an arrival, and let $\mathcal{D} = \mathbf{I}_0 - \mathbf{I}_{0+}$ denotes the decrease of the interference arisen by a departure. Thus we get:

$$\lambda|\mathbf{S}|\mathbb{E}^{\uparrow}[\mathcal{I}] = \lambda_d\mathbb{E}^{\downarrow}[\mathcal{D}] \tag{21}$$

Where $\mathbb{E}^{\uparrow}$ and $\mathbb{E}^{\downarrow}$ are the palm probabilities at the time of arrival or departure. Combing (21) with (19), we know that:

$$\mathbb{E}^{\uparrow}[\mathcal{I}] = \mathbb{E}^{\downarrow}[\mathcal{D}] \tag{22}$$

By applying the Campbell's theory, we get:

$$\mathbb{E}^{\uparrow}[\mathcal{I}^{BF}] = 2\mathbb{E}[\sum_{x\in\Phi_0} G_{ox}^T G_{ox}^R P\ell(\|x\|)] \tag{23}$$

$$= 2P\frac{\mathbb{E}[\Phi_0(\mathbf{S})]}{|\mathbf{S}|}\mathbb{E}[\int_{\mathbf{S}} G_{ox}^T G_{ox}^R \ell(\|x\|)dx] \tag{24}$$

Where G_{ox}^T and G_{ox}^R are the antenna gains between the receiver at origin and the interfering transmitter at x. Let $a^{BF} = \int_{\mathbf{S}} G_{ox}^T G_{ox}^R \ell(\|x\|)$. Since the position of interfering devices are uniformly distributed in the plane, and the antenna gain G_{ox}^T and G_{ox}^R are independent, we get the expression of $\mathbb{E}[\hat{a}^{BF}]$ in (13). For a stationary process, the departure rate λ_d follows the Papangelou's theorem [17]:

$$\lambda_d\mathbb{E}^{\downarrow}[\mathcal{D}] = \mathbb{E}[\lambda_d(0)\mathcal{D}] \tag{25}$$

Let $\mathbf{R}_0^{BF} = \sum_{x\in\Phi_0} R^{BF}(x,\Phi_0)$. We can then get the expression of $\mathbb{E}^{\downarrow}[\mathcal{D}]$ as follows:

$$\mathbb{E}^{\downarrow}[\mathcal{D}] = 2\mathbb{E}\left[\frac{\lambda_d(0)}{\lambda_d}\sum_{x\in\Phi_0}\frac{R^{BF}(x,\Phi_0)}{\boldsymbol{R}_0^{BF}} I^{BF}(x,\Phi_0)\right] \tag{26}$$

$$= 2\frac{\mathbb{E}[\sum_{x\in\Phi_0} R^{BF}(x,\Phi_0)I^{BF}(x,\Phi_0)]}{\mathbb{E}[\boldsymbol{R}_0^{BF}]} \tag{27}$$

$$= 2\frac{\mathbb{E}_{\Phi_0}^0[R^{BF}(0,\Phi_0)I^{BF}(0,\Phi_0)]}{\mathbb{E}[\boldsymbol{R}_0^{BF}]}\mathbb{E}[\Phi_0(\mathbf{S})] \tag{28}$$

Adapting (24) and (28) to (22), we get:

$$2P\frac{\mathbb{E}[\Phi_0(\mathbf{S})]}{|\mathbf{S}|}\mathbb{E}[a^{BF}] = 2\frac{\mathbb{E}_{\Phi_0}^0[R^{BF}(0,\Phi_0)I^{BF}(0,\Phi_0)]}{\mathbb{E}[\boldsymbol{R}_0^{BF}]}\mathbb{E}[\Phi_0(\mathbf{S})] \tag{29}$$

By applying (20) to (29), we obtain:

$$\lambda = \frac{\mathbb{E}_{\Phi_0}^0[R^{BF}(0,\Phi_0)I^{BF}(0,\Phi_0)]}{PL\mathbb{E}[a^{BF}]} \tag{30}$$

Given the definition of the transmission rate in (10), we have:

$$R^{BF}(0,\Phi_0)I^{BF}(0,\Phi_0) \le \frac{PBg_a^T(\xi,\theta_0^T)g_a^T(\psi,\theta_0^R)\ell(T)}{\ln(2)} \tag{31}$$

Combing (30) and (31), we get the following inequality:

$$\lambda \le \frac{B\mathbb{E}[g_a^T(\xi,\theta_0^T)]\mathbb{E}[g_a^T(\psi,\theta_0^R)]\ell(T)}{\ln(2)L\mathbb{E}[a^{BF}]}. \tag{32}$$

REFERENCES

[1] R. Wang, N. Deng, and H. Wei, "Towards a deep analysis of millimeter wave d2d underlaid cellular networks," *IEEE Transactions on Communications*, pp. 1–1, 2021.

[2] E. Turgut and M. C. Gursoy, "Uplink performance analysis in d2d-enabled millimeter-wave cellular networks with clustered users," *IEEE Transactions on Wireless Communications*, vol. 18, no. 2, pp. 1085–1100, 2019.

[3] Y. Quan, J.-M. Kelif, and M. Coupechoux, "Spatio-temporal wireless d2d network with beamforming," *IEEE International Conference on Communications (ICC)*, June 2021.

[4] M. Salehi, A. Mohammadi, and M. Haenggi, "Analysis of d2d underlaid cellular networks: Sir meta distribution and mean local delay," *IEEE Transactions on Communications*, vol. 65, no. 7, pp. 2904–2916, 2017.

[5] X. Lu, M. Salehi, M. Haenggi, E. Hossain, and H. Jiang, "Stochastic geometry analysis of spatial-temporal performance in wireless networks: A tutorial," *IEEE Communications Surveys Tutorials*, pp. 1–1, 2021.

[6] P. D. Mankar, M. A. Abd-Elmagid, and H. S. Dhillon, "Spatial distribution of the mean peak age of information in wireless networks," *IEEE Transactions on Wireless Communications*, vol. 20, no. 7, pp. 4465–4479, 2021.

[7] R. Rao and A. Ephremides, "On the stability of interacting queues in a multiple-access system," *IEEE Transactions on Information Theory*, vol. 34, no. 5, pp. 918–930, 1988.

[8] A. Sankararaman and F. Baccelli, "Spatial birth–death wireless networks," *IEEE Transactions on Information Theory*, no. 6, pp. 3964–3982, June 2017.

[9] C. Preston, "Spatial birth and death processes," *Advances in applied probability*, vol. 7, no. 3, pp. 465–466, 1975.

[10] N. Bahadori, N. Namvar, B. Kelleyy, and A. Homaifar, "Device-to-device communications in millimeter wave band: Impact of beam alignment error," in *2019 Wireless Telecommunications Symposium (WTS)*, 2019, pp. 1–6.

[11] M. Wang, C. Zhang, X. Chen, and S. Tang, "Performance analysis of millimeter wave wireless power transfer with imperfect beam alignment," *IEEE Transactions on Vehicular Technology*, vol. 70, no. 3, pp. 2605–2618, 2021.

[12] M. S. Zia, D. M. Blough, and M. A. Weitnauer, "Coverage in millimeter-wave networks with snr-dependent beam alignment errors," in *2020 IEEE 91st Vehicular Technology Conference (VTC2020-Spring)*, 2020, pp. 1–5.

[13] J. D. Kraus and R. J. Marhefka, *Antenna for all applications*. McGraw-Hill, 2002.

[14] H. J. Visser, *Array and Phased Array Antenna Basics: Palm Martingale Calculus and Stochastic Recurrences*. Wiley, 2006.

[15] N. L. Johnson, S. Kotz, and N. Balakrishnan, *Continuous Univariate Distributions, Volume 1, 2nd Edition*. John Wiley and Sons, 1994.

[16] M. Miyazawa, "Rate conservation laws: A survey," *Queueing Systems*, vol. 15, pp. 1–58, March 1994.

[17] F. Baccelli and P. Bremaud, *Elements of Queueing Theory:Palm Martingale Calculus and Stochastic Recurrences*. Springer, 2003.